International Journal of Automotive Technology, Vol. 13, No. 4, pp. 583−592 (2012)
DOI 10.1007/s12239−012−0056−x

pISSN 1229−9138/ eISSN 1976-3832

ACTIVELY TRANSLATING A REAR DIFFUSER DEVICE FOR THE AERODYNAMIC DRAG REDUCTION OF A PASSENGER CAR

S. O. KANG[1)], S. O. JUN[2)], H. I. PARK[1)], K. S. SONG[1)], J. D. KEE[1,3)], K. H. KIM[1,4)] and D. H. LEE[1,4)*]

[1)]School of Mechanical and Aerospace Engineering, Seoul National University, Seoul 151-744, Korea
[2)]BK21 School for Creative Engineering Design for Next Generation Mechanical and Aerospace System, Seoul National University, Seoul 151-744, Korea
[3)]Research Development Division, Hyundai Motors Company, 772-1 Jangdeog-dong, Hwaseong-si, Gyeonggi 445-706, Korea
[4)]School of Mechanical and Aerospace Engineering, Institute of Advanced Aerospace Technology, Seoul National University, Seoul 151-744, Korea

(Received 8 August 2011; Revised 8 November 2011; Accepted 23 December 2011)

ABSTRACT−This research aims to develop an actively translating rear diffuser device to reduce the aerodynamic drag experienced by passenger cars. One of the features of the device is that it is ordinarily hidden under the rear bumper but slips out backward only under high-speed driving conditions. In this study, a movable arc-shaped semi-diffuser device, round in form, is designed to maintain the streamlined automobile's rear underbody configuration. The device is installed in the rear bumper section of a passenger car. Seven types of rear diffuser devices whose positions and protrusive lengths and widths are different (with the basic shape being identical) were installed, and Computational Fluid Dynamics (CFD) analyses were performed under moving ground and rotating wheel conditions. The main purpose of this study is to explain the aerodynamic drag reduction mechanism of a passenger car cruising at high speed via an actively translating rear diffuser device. The base pressure of the passenger car is increased by deploying the rear diffuser device, which then prevents the low-pressure air coming through the underbody from directly soaring up to the rear surface of the trunk. At the same time, the device generates a diffusing process that lowers the velocity but raises the pressure of the underbody flow, bringing about aerodynamic drag reduction. Finally, the automobile's aerodynamic drag is reduced by an average of more than 4%, which helps to improve the constant speed fuel efficiency by approximately 2% at a range of driving speeds exceeding 70 km/h.

KEY WORDS : Automobile aerodynamics, Active rear diffuser device, Drag reduction, Fuel efficiency improvement

1. INTRODUCTION

Because oil prices have doubled in the last ten years and because government regulations regarding CO_2 emissions are becoming more severe, the need to improve the fuel efficiency of automobiles has become a key topic in the automobile technology field. Fuel efficiency is dependent on many parameters of an automobile, including its engine, transmission, auxiliary load, brakes, vehicle weight, tires, aerodynamic drag, and the driving habits of the driver. Considering the endeavors of many scientists and engineers, there have been advances in all areas of automobile design in recent decades.

Nevertheless, automobile aerodynamics has been considered less important compared with other areas, as a car does not use aerodynamic force as a power source, as an airplane does, but instead only runs on the ground. Moreover, an aerodynamically efficient shape can alter the aesthetic external configuration design of an automobile, which may be the most important factor for people who want glamorous and fancy merchandise. For these reasons, efforts to reduce the aerodynamic drag of an automobile have comparably less influence than those on powertrain efficiency or weight reduction to improve fuel efficiency.

However, as automobile technology develops, the speed of automobiles is increasing. Thus, the aerodynamic performance becomes crucial because aerodynamic drag is proportional to the square of the speed. Additionally, a reduction of the aerodynamic drag is achievable at a relatively low cost compared with developing a more efficient powertrain system (Howell *et al*., 2002), which means it is highly economical technology.

Different from an airplane wing, an automobile has a streamlined shape at the front, but an angulated bluff shape at the back. This design causes highly complex and abstruse rear flow patterns, such as eddies, vortices, up-wash, down-

**Corresponding author.* e-mail: donghlee@snu.ac.kr

wash and mixed wake flows (Kee *et al*., 2001). Therefore, controlling the rear flow of an automobile is a core technology that can improve the aerodynamic performance.

Numerous studies have been performed in an attempt to reduce automotive aerodynamic drag via the passive or active flow control of the rear wake of the car. Among the solutions reviewed in previous studies for passive flow control, Gillieron and Kourta (2009) proposed the use of splitter plates as a type of drag reduction for a simplified form of car geometry. Beaudoin and Aider (2008) presented an experimental study of flow control using flaps over a classic 3D bluff-body and achieved a level of drag reduction. Ha *et al*. (2011) performed a study of the drag reduction of a pickup truck using rear flaps. Singh (2003) developed an aerodynamic design optimization process for an automotive vehicle that changes the shape of the trunk to achieve a reduction of drag.

For active flow control, Geropp and Odenthal (2000) performed a jet-blowing experiment to increase the base pressure of a car-shaped body to obtain a reduction of drag. Wassen *et al*. (2010) performed experimental and numerical investigations aiming at the reducing the total aerodynamic drag of a generic car model by means of active separation control. Leclerc and Levallois (2006) used an active synthetic jet control technique to obtain an innovative flow control solution capable of significantly reducing vehicle fuel consumption.

However, with passive flow control, an additional flap or plate must be installed, which alters the aesthetic aspect of the streamlined external automobile shape. Furthermore, the external configuration of the automobile, as developed by the aesthetic designer, cannot be simply modified only for better aerodynamic efficiency. With active flow control, complex equipment should be installed to activate blowing or suction, and an additional energy source should be used to control the rear flow, which is highly impractical when applied to commercial automobiles.

To solve these problems of passive or active flow control and to achieve the aerodynamic drag reduction of a passenger car, an actively translating rear diffuser device is suggested in this study. The device is hidden under the rear bumper of a passenger car when it is parked and at low driving speeds so as not to alter the aesthetic design of the car. Only at high speeds (above 70 km/h) does the rear diffuser device slip out and therefore change the automobile's rear flow pattern. In an actual driving condition with moving ground and rotating wheels, aerodynamic drag is reduced by blocking out the low-pressure air from the under flow of the automobile and generating a diffuser effect, which serves to raise the base pressure of the passenger car.

The main purpose of this study is to investigate the drag reduction phenomenon of a passenger car induced by a rear diffuser device according to the diffuser length and the driving speed condition. A physical explanation for this drag reduction mechanism is also given.

2. BACKGROUND

2.1. Actively Translating Rear Diffuser Device

Numerous studies and experiments have shown that the dominant fluid motion over the rear area of an automobile and its wake are highly correlated with the flow coming through its underbody (Song *et al*., 2006). This dynamic implies that it may be possible to modify the flow behind the passenger vehicle by controlling the flow through the underbody. Considering the rear under configuration of the automobile itself, passenger cars have a diffuser shape between the road and the rear underbody (Song *et al*., 2010). Aerodynamically, the diffuser increases the pressure and decreases the velocity of the air flow. Potthoff demonstrated an experiment on a simplified car body showing that automobile drag is affected by the diffuser area ratio (diffuser outlet area/diffuser inlet area) and the diffuser's length (Potthoff, 1982; Hucho, 1998). It was observed that drag reduction is achieved through the diffuser effect, resulting in an increase of the base pressure of the car body. Based on this concept of the diffuser effect, an actively translating rear diffuser device is suggested in this study, where a movable arc-shaped diffuser device is installed under the rear bumper of the passenger car. The device is rounded to maintain a smooth, streamlined rear underbody shape to obtain a greater diffusion effect when it is fully extracted. The basic concept of the actively translating rear diffuser device is shown in Figure 1. This device is hidden under the rear bumper while the car is parked and during low-speed driving, when the aerodynamic drag is negligible, because it is important not to alter the aesthetic design of the external configuration. Only at high speeds (above 70 km/h) does the rear diffuser device become active and control the rear flow of the automobile to reduce the aerodynamic drag.

Once the rear diffuser device slides from its rear bumper position, the rear flow and wake patterns of the passenger car change significantly. Figure 2 shows comparisons of the streamline between the baseline condition and when the rear diffuser is in use at three different angles. A strong flow pattern from the underbody is observed to increase sharply to the rear surface of the trunk in the baseline

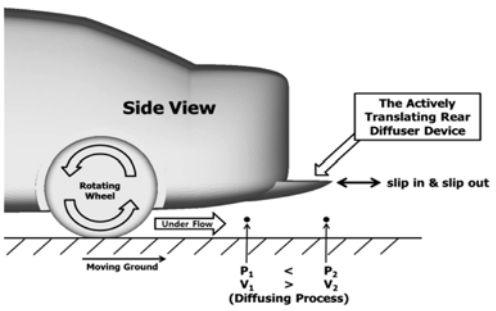

Figure 1. Basic concept of the actively translating rear diffuser device.

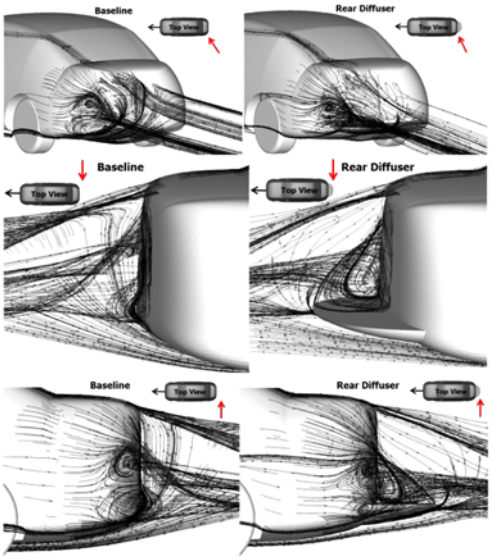

Figure 2. Streamline comparison at three different angles.

condition, but this flow is blocked when the rear diffuser is active. When the device is active, the rear surface area of the trunk contains the side and upper flow instead of the underbody flow.

2.2. CFD ANALYSIS

2.2.1. Modeling of passenger car configuration

In this study, the Vehicle Modeling Function (VMF) as suggested by Rho *et al*. (2008, 2009; Kang *et al*., 2009, 2010a, 2010b) is used to realize a three-dimensional virtual passenger car configuration. This concept is demonstrated in Figure 3. The approximated three-dimensional passenger car model used in this study for the baseline condition is shown in Figure 4.

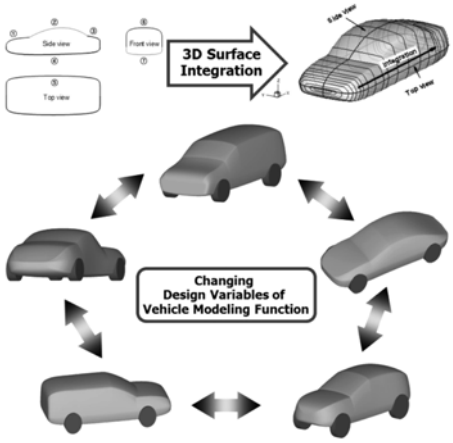

Figure 3. Automobile configuration formation using VMF.

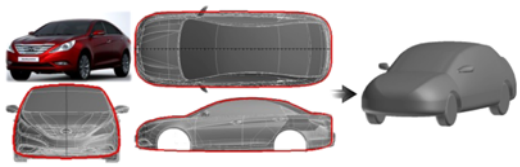

Figure 4. Realizing a passenger car configuration using VMF.

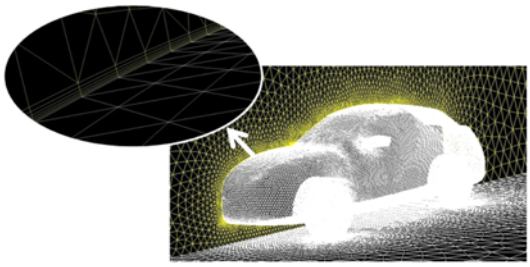

Figure 5. Triangular boundary surface mesh (95,210 faces).

2.2.2. Grid generation for CFD simulation

Because an automobile has a symmetric configuration, only half of the passenger car model is used to reduce computational time cost. In addition, triangular surface meshes are used to create an unstructured grid system, as shown in Figure 5.

There are nearly 95,000 surface meshes for every case. To catch the boundary layer from the wall surface, six prism layers in a boundary of 6.5 mm are piled from the automobile wall surface, completing the 3D volume meshes. The boundary prism layers and the volume mesh configuration are shown in Figure 6. There are approximately 820,000 volume meshes for every case.

2.2.3. Grid independence test

In CFD research, the number of cells in the computational domain can affect the result of the analysis. Therefore, a grid independence test is indispensible. After an iterative test of the number of cells, a mesh of approximately 820,000 cells was chosen as the standard level of the grid

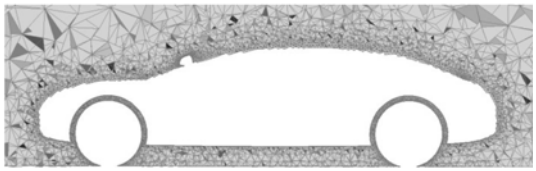

Figure 6. Boundary prism and volume mesh (821,508 cells).

Table 1. Grid independence test.

Total number of cells	C_D	Convergence time
650,000	0.2901	5 hours
760,000	0.2854	7 hours
820,000	0.2823	10 hours
1,000,000	0.2823	16 hours

fineness in terms of accuracy and computational time. Table 1 shows the results of the grid independence test.

2.2.4. Boundary conditions for the CFD analysis

To simulate a passenger car moving on an actual road, the computational domain was set up as shown in Figure 7. The dimension of the computational domain is chosen such that the aerodynamic force is not affected by the domain size (Song *et al*., 2011). Although numerous studies have investigated aerodynamic drag reduction on the configuration of a car, most did not consider the moving ground and rotating wheel effects, which have a critical effect on the automobile's rear flow characteristics. Given the moving ground and rotating wheel conditions, it is known that a sedan shows quite different aerodynamic characteristics from that on stationary ground and under a stationary wheel condition (Le Good *et al*., 1998; Elofsson and Bannister, 2002). Therefore, every numerical simulation in this study was performed under the moving ground and rotating wheel conditions. The angular velocities of the rotating wheels and the speed of the moving ground were set according to the driving speed. Both parameters are summarized in Table 2, and the overall boundary conditions for the CFD analysis are shown in Figure 8.

2.2.5. Methodology for CFD analysis

In this study, the commercial CFD solver ANSYS

Table 2. Driving speed and wheel and ground conditions for the CFD analysis.

Driving speed		Rotating wheels	Moving ground
(km/h)	(m/s)	(rad/s)	(m/s)
70	19.44	59.73	19.44
85	23.61	72.53	23.61
100	27.78	85.34	27.78
115	31.94	98.12	31.94
130	36.11	110.94	36.11
145	40.28	123.74	40.28
160	44.44	136.53	44.44

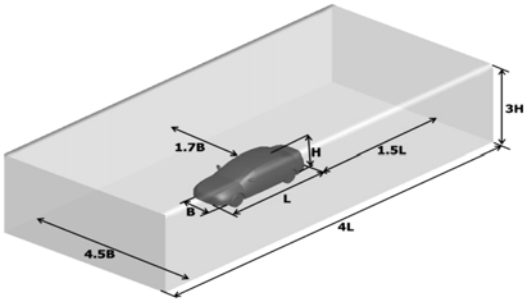

Figure 7. Dimensions of the computational domain.

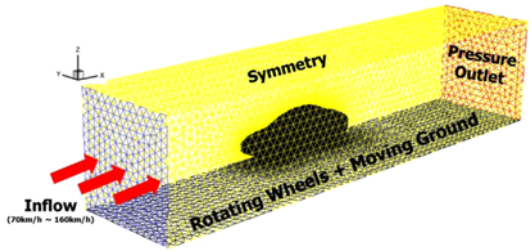

Figure 8. Boundary conditions for the CFD analysis.

FLUENT was used. In the course of the analysis, a coupled equation system using a preconditioning method is used to improve the convergence performance. A second-order upwind difference scheme is used as the main scheme to solve the Navier-Stokes equations, and DES (Detached Eddy Simulation) is used as the turbulence model. To overcome the deficiencies of RANS models for predicting massively separated flows, Spalart *et al*. (1997) proposed DES with the objective of developing a numerically feasible and accurate approach combining the most favorable elements of RANS models and Large Eddy Simulation (LES). Kapadia *et al*. (2003) showed clearly that DES is able to resolve the flow details better than the RANS mode for the same time step. DES is a hybrid turbulence model that combines features of RANS simulation in the near wall regions and LES in the region where large turbulence scales play a dominant role (Favre *et al*, 2010, Islam *et al*, 2009). A realizable k-e model is chosen in the vicinity of walls because it is known to provide superior performance for flows involving rotation, boundary layers under adverse pressure gradients, separation and recirculation. Singh *et al*. (2004) performed a validation of four turbulence models (Spalart-Allmaras, Standard k-e, Renormalization-group k-e, and Realizable k-e) integrated in FLUENT and proved that a realizable k-

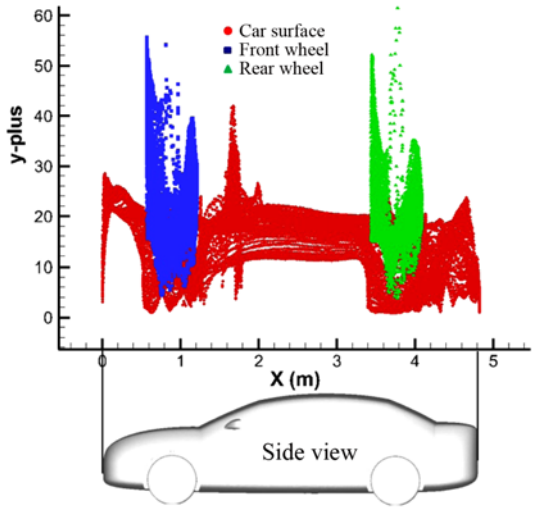

Figure 9. y+ plot for the car and tire wall surfaces.

Table 3. Specific information for numerical procedure.

Scheme	Pressure-velocity coupling	
Courant number	1	
Explicit relaxation factor	Momentum	0.5
	Pressure	0.5
	Density	0.5
	Body forces	1
Under-relaxation factor	Turbulent kinetic energy	0.8
	Turbulence dissipation rate	0.8
	Turbulent viscosity	0.8
	Energy	0.5
Discretization	Pressure	Standard
	Momentum	Second order upwind
	Turbulent kinetic energy	Second order upwind
	Turbulence dissipation rate	Second order upwind
	Energy	Second order upwind
Running time	More than 10 hours	
Capacity of computer	16 node parallel cluster (Intel Quad Core Xeon E3320 2.5 GHz)	
Convergence criterion	Residual of continuity <1e-04	

e model gives the best match with the experimental results.

Figure 9 shows the range of y+ values around the car and tire wall surfaces. The y+ values are mostly in the range of 10~25; therefore, the law of wall can be applied, and the realizable k-e model, which uses the standard wall functions, is available at the wall surfaces.

The automotive aerodynamic simulation condition is fully turbulent (Re > 8·10E6), and the moving ground and rotating wheel conditions cause the turbulence intensity to have a large value. The turbulence intensity at the inlet and outlet boundaries is set as 2% based on a reference in which a numerical study of moving ground vehicles was performed (Diedrichs, 2003). Specific information for the numerical procedure is summarized in Table 3 (Yun, 2004).

Finally, all C_D values for a passenger car with seven types of rear diffusers are evaluated through steady analysis solutions that are fully converged.

3. RESULT AND DISCUSSION

3.1. Modeling of Rear Diffuser Device

Seven types of diffuser devices with differing positions, protrusive length, width and height (but the same basic shape) were constructed for assessment in a CFD analysis.

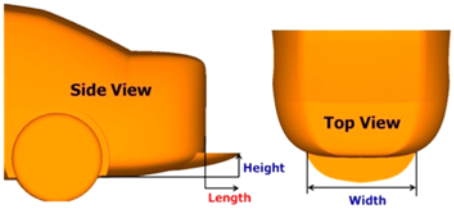

Figure 10. Definition of the rear diffuser size.

Table 4. Specifications of the seven rear diffusers.

	Length (mm)	Width (mm)	Height (mm)
Case 1	100	1518.2	144.5
Case 2	200	1318.2	154.5
Case 3	300	1218.2	174.5
Case 4	350	1218.2	194.5
Case 5	400	1218.2	204.5
Case 6	450	1158.2	224.5
Case 7	500	1078.2	244.5

The length, width and height are shown in Figure 10, and the specifications of the rear diffuser are demonstrated in Table 4.

The maximum length of the rear diffuser device was set at 500 mm due to the storage constraint. The passenger car configuration developed in this study has a 500 mm trunk length; above this length, the diffuser device may have to be folded or bent. Except for the different configurations of the rear diffuser devices, all other factors in the automobile configuration and analysis conditions were identical. Figure 11 shows seven automobile configuration cases with the actively translating rear diffuser device compared with the baseline model for the CFD analysis.

3.2. Aerodynamic Drag Analysis of Passenger Car with Rear Diffuser Device

The aerodynamic performance of an automobile is estimated by measuring the drag force acting on the external car surface. However, each automobile has a different configuration, meaning that the drag force needs

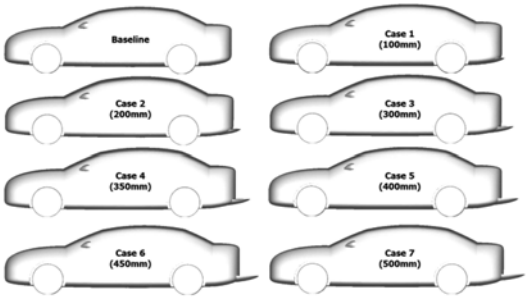

Figure 11. Seven rear diffuser cases (side view).

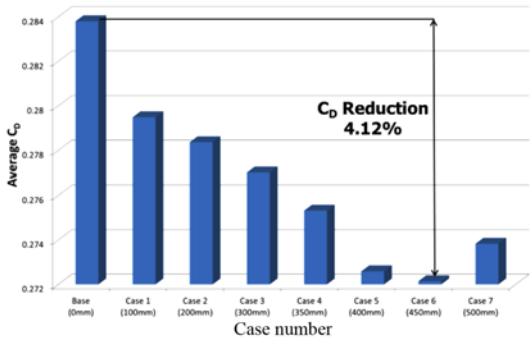

Figure 12. Average C_D according to the case number.

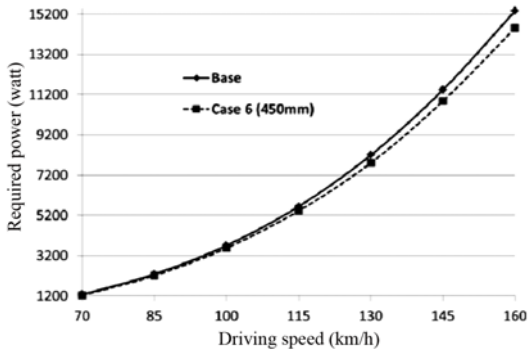

Figure 13. Required power to overcome the aerodynamic drag (Base & Case 6).

to be normalized to compare one to another. The drag coefficient C_D is regarded as a major indicator that represents the aerodynamic performance of an automobile. Table 5 demonstrates the C_D values from the seven different cases and the baseline case at seven different driving speeds. The average C_D values are also shown in the last row to compare the drag reduction effect according to the size of the rear diffuser device. As shown in Table 5, irrespective of the size of the rear diffuser device and the driving speed (70 km/h ~ 160 km/h), every diffuser device induces some C_D reduction effects in the automobile. Moreover, as the length of the diffuser increases, the C_D reduction effect also increases. Here, Case 6 (450 mm) shows the most effective C_D reduction rate, at a value of approximately 4.12%, compared with the baseline, as displayed in Figure 12. Focusing on Case 6, the drag reduction effect of the rear diffuser shows an increase as the driving speed increases, as confirmed in Figures 13. The gap in the required power to overcome the aerodynamic drag force between the baseline and Case 6 becomes wider as the driving speed increases, which indicates that the rear diffuser device is more useful as the automobile travels faster.

3.3. Drag Reduction Mechanism Induced by the Rear Diffuser Device

3.3.1. Blocking the underbody flow

To investigate why the drag reduction mechanism is induced by the rear diffuser device, the pressure distribution contour of the baseline condition was analyzed, as shown in Figure 14. Focusing on the rear body area, the pressure difference appears at the upper flow, the side flow and the under flow. The pressure of the upper flow is the highest, with that of the side flow second and that of the under flow third. As observed in Figure 15, the most evident characteristic of the streamline pattern in the baseline condition is the strong upwash flow that soars up the rear side of the trunk. However, the extracted rear diffuser device blocks out the upwash from the bottom. The space behind the rear trunk surface, which is supposed to be filled with the underbody flow, is instead filled with the side flow and the upper flow passing over the trunk.

Therefore, the drag reduction phenomenon is explained in terms of a blocking out of the low-pressure air in its position behind the trunk surface, allowing for relatively high-pressure air from the side and the upper position of the trunk. Finally, the base pressure is increased, which

Table 5. Analysis results: C_D of the passenger car.

Driving speed (km/h)	Baseline (0 mm)	Case 1 (100 mm)	Case 2 (200 mm)	Case 3 (300 mm)	Case 4 (350 mm)	Case 5 (400 mm)	Case 6 (450 mm)	Case 7 (500 mm)
	C_D	C_D	C_D	C_D	C_D	C_D	C_D	C_D
70	0.2822	0.281	0.2782	0.2771	0.276	0.2753	0.2749	0.2754
85	0.2828	0.2794	0.2783	0.2765	0.2747	0.2743	0.2741	0.2746
100	0.2823	0.2789	0.2771	0.2756	0.2740	0.2729	0.2726	0.2741
115	0.2831	0.2784	0.2778	0.2771	0.2764	0.2731	0.2721	0.2736
130	0.2844	0.2779	0.2774	0.2768	0.2759	0.2709	0.2708	0.2732
145	0.286	0.2794	0.2786	0.2778	0.2752	0.2709	0.2705	0.2734
160	0.2858	0.2814	0.2812	0.2782	0.275	0.2707	0.27	0.2725
Average	0.2838	0.2795	0.2784	0.2770	0.2753	0.2726	0.2721	0.2738

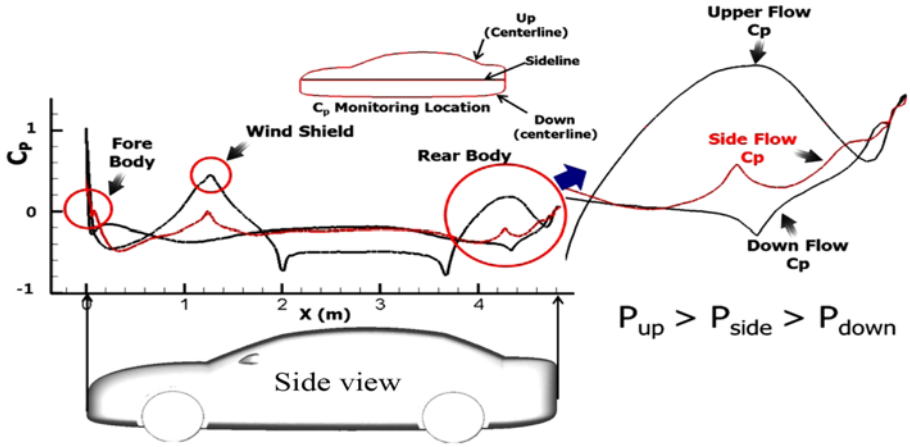

Figure 14. Pressure distribution along the centerline and the sideline of the baseline.

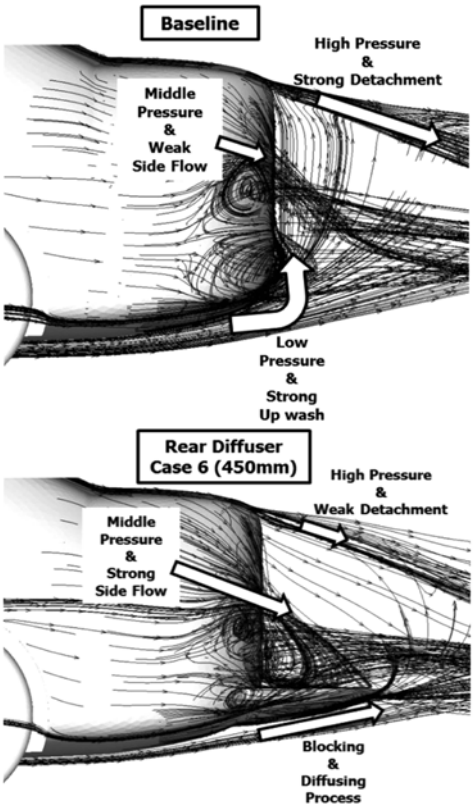

Figure 15. Schematic description of the drag reduction mechanism.

results in the reduction of aerodynamic drag.

3.3.2. Generating the diffuser effect

To identify the diffuser effect, which increases the pressure of the flow, the pressure distribution contours along the centerline of a passenger car with the rear diffuser device employed at a speed of 130 km/h were assessed, as demonstrated in Figure 16. Once the rear diffuser device slides out from under the rear bumper, the pressure contour line around the rear body is shifted to the upper position compared with the baseline. This shift occurs because the total length of the car is extended, causing a different pressure distribution pattern to appear. Then, as the diffuser becomes longer, the pressure increase effect grows stronger because the longer diffuser device induces an extended pressure-raising process. In Figure 16, the C_D values according to the case number (Baseline, Case 2, Case 4, Case 6) are also indicated. These findings confirm that the drag reduction effect increases as the diffuser length increases. Case 6 (450 mm) shows the best performance.

At 130 km/h, a drag reduction of up to 4.78% compared with the baseline condition is achieved in Case 6. The maximum drag reduction is as high as 5.53% in Case 6 at 160 km/h, as confirmed in Table 5. Figure 17 demonstrates the base pressure distribution of the trunk surface. It was found that the base pressure in all the cases increases compared with the baseline condition and that the base pressure distribution on the rear surface changes according to the diffuser length. Case 6 has the largest high-pressure area, implying that it has the highest base pressure among all cases. In Figure 18, the pressure contour plane downstream also proves that the base pressure is increased considerably by the diffuser device.

However, the simulation result shows that the drag reduction effect by the rear diffuser in Case 7 (500 mm) is lower than that of Case 6 (450 mm), indicating that the optimum length of the diffuser is approximately 450 mm. In other words, the optimal length, position and shape of the rear diffuser device needed to obtain the device's optimal configuration is saved for future work.

3.3.3. Generation of lift force

As the results indicate, the rear diffuser device increases the pressure force on the underbody surface, which could cause a decreasing downward aerodynamic force, which means that the device could cause driving instability. However, as summarized in Table 6, only 1.5% (4.4 N) of the lift force is increased by the rear diffuser device even at

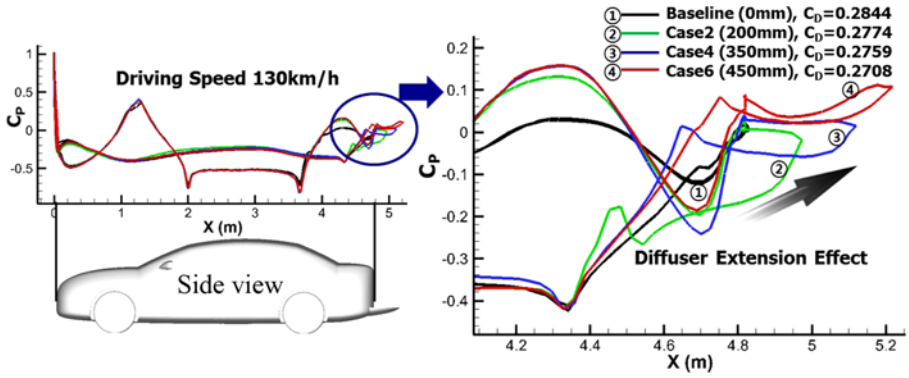

Figure 16. Pressure distribution along the centerline when the rear diffuser device exists.

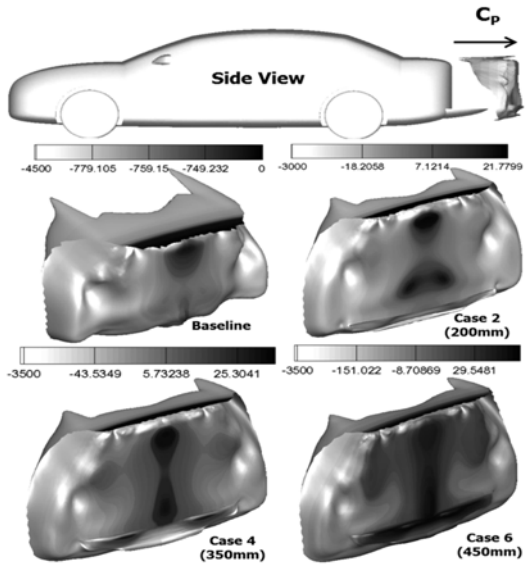

Figure 17. Pressure contour on the rear surface.

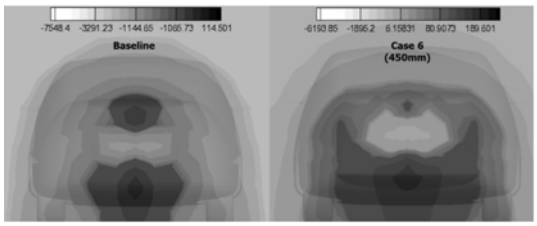

Figure 18. Pressure contour plane downstream.

Table 6. Lift force analysis of the passenger car.

	Baseline	Case 6 (450 mm)
Lift Force (at 160 km/h)	295.3 N (30.13 kgf)	299.7 N (30.58 kgf)
Increment	1.5% ↑, 4.4 N (0.45 kgf)	

the highest speed (160 km/h), an increase that is negligible. Therefore, the device does not incur the driving instability problem.

3.4. Fuel Efficiency Improvement through Aerodynamic Drag Reduction

The ultimate purpose of aerodynamic drag reduction in an automobile is to improve the fuel efficiency. In this study, an average aerodynamic drag reduction of more than 4% is achieved by an actively translating rear diffuser device, which is a clear improvement of the fuel efficiency.

Advisor (Advanced Vehicle Simulator), which was developed by the National Renewable Energy Laboratory (www.nrel.gov), was used here to estimate the effects of the aerodynamic drag of a passenger car on its fuel efficiency. There are several modes that can be used to estimate the fuel efficiency of an automobile, but the constant speed mode was used here for a good degree of agreement with the analysis results from the constant speed driving condition. All the variables related to such parts as the power train and the transmission were set to their default values, except for the fluctuating aerodynamic drag variable when Advisor was used. The estimated fuel efficiency is summarized in Table 7 according to the C_D values. Compared with the baseline condition, the maximum fuel efficiency improvement is as high as 2.21% in Case 6, with the average values given for comparison. Figure 19 shows an average fuel efficiency histogram, demonstrating that fuel efficiency improvement can be achieved through aerodynamic drag reduction.

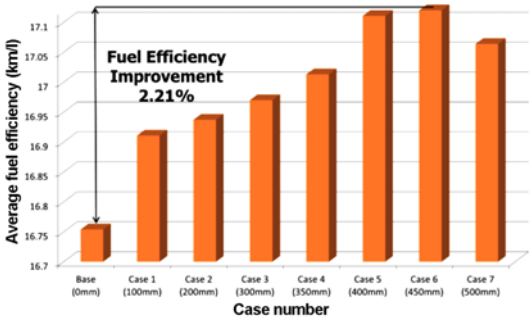

Figure 19. Average fuel efficiency in constant speed mode according to the case number.

Table 7. Fuel efficiency in constant speed mode based on C_D.

Driving speed (km/h)	Baseline (0 mm)	Case 1 (100 mm)	Case 2 (200 mm)	Case 3 (300 mm)	Case 4 (350 mm)	Case 5 (400 mm)	Case 6 (450 mm)	Case 7 (500 mm)
	Fuel efficiency (km/l)	Fuel efficiency (km/l)	Fuel efficiency (km/l)	Fuel efficiency (km/l)	Fuel efficiency (km/l)	Fuel efficiency (km/l)	Fuel efficiency (km/l)	Fuel efficiency (km/l)
70	24.45	24.46	24.48	24.49	24.50	24.50	24.51	24.50
85	22.75	22.84	22.87	22.92	22.97	22.98	22.99	22.98
100	20.63	20.71	20.76	20.80	20.84	20.868	20.88	22.84
115	18.96	19.22	19.23	19.25	19.26	19.34	19.36	19.33
130	15.57	15.89	15.91	15.94	15.99	16.25	16.25	16.13
145	10.87	11.13	11.18	11.22	11.36	11.59	11.61	11.45
160	4.06	4.13	4.13	4.17	4.18	4.24	4.25	4.21
Average	16.75	16.91	16.94	16.97	17.01	17.11	17.12	17.06

4. CONCLUSIONS

In this study, an actively translating rear diffuser device is proposed for automotive aerodynamic drag reduction. The performance of the device was tested through a CFD simulation. From the results, the following conclusions can be made:

(1) Once the rear diffuser device slides out from under the rear bumper, the aerodynamic drag of the passenger car is reduced within the speed range of 70 km/h~160 km/h. Among the various lengths of the diffuser, Case 6 (450 mm) showed the best drag reduction performance, with an average reduction of more than 4%. Moreover, as the driving speed increases, the drag reduction effect also increases.

(2) The automobile drag reduction mechanism is explained as follows. The diffuser device blocks out the low-pressure air from the underbody and allows relatively high-pressure air from the sides and the upper part of the trunk to fill the space behind the trunk, which results in an increase in the base pressure. According to its configuration, the device generates a diffusion effect that increases the underbody flow pressure, thus heightening the base pressure of the car body.

(3) An improvement of fuel efficiency is achieved through aerodynamic drag reduction using the actively translating rear diffuser device when the passenger car is travelling at a high speed.

Obtaining the optimal configuration of the actively translating rear diffuser device through an optimization process is saved for future work.

ACKNOWLEDGEMENT–This work was accomplished by the supports of the project named Industrial Strategic Technology Development Program (10033753-2010-12) which is funded by the Ministry of Knowledge Economy (MKE, Korea), the New and Renewable Energy Program of the Korea Institute of Energy Technology Evaluation and Planning (KETEP) grant funded by the Korea government Ministry of Knowledge Economy (No.20104010100490), the National Research Foundation of Korea (NRF) grant funded by the Korea government (MEST) (No. 20110001227), the sixth stage of the Brain Korea 21 Project in 2011 by School for Creative Engineering Design of Next Generation Mechanical and Aerospace Systems at Seoul National University of the Korean Ministry of Education, Science and Technology.

REFERENCES

Beaudoin, J. and Aider, J. (2008). Drag and lift reduction of a 3D bluff body using flaps. *Exp Fluid*, **44**, 491–501.

Diedrichs, B. (2003). On computational fluid dynamics modeling of crosswind effects for high-speed rolling stock. *Proc. Institution of Mechanical Engineers*, *Part F*, *J. Rail and Rapid Transit*.

Elofsson, P. and Bannister, M. (2002). Drag reduction mechanisms due to moving ground and wheel rotation in passenger cars. *SAE Paper No.* 2002-01-0531.

Favre, T., Diedrichs, B. and Efraimsson, G. (2010). Detached-eddy simulations applied to unsteady crosswind aerodynamics of ground vehicles. *Notes on Numerical Fluid Mechanics and Multidisciplinary Design*, **111**, *Progress in Hybrid RANS-LES Modeling*, 167–177.

Fluent Inc. (2006). Fluent 6.3 User'S Guide.

Geropp, D. and Odenthal, H. -J. (2000). Drag reduction of motor vehicles by active flow control using the COANDA effect. *Experiments in Fluids* **28**, **1**, 74–85.

Gillieron, P. and Kourta, A. (2009). Aerodynamic drag reduction by vertical splitter plates. *Exp. Fluids.* **48**, **1**, 1–16.

Ha, J. S., Jeong, S. and Obayashi, S. (2011). Drag reduction of a pickup truck by a rear downward flap. *Int. J. Automotive Technology* **12**, **3**, 369–374.

Howell, J., Sherwin, C., Passmore, M. and Le Good, G.

(2002). Aerodynamic drag of a compact SUV as measured on-road and in the wind tunnel. *SAE Paper No.* 2002-01-0529.

Hucho, W. (1998). *Aerodynamics of Road Vehicles from Fluid Mechanics to Vehicle Engineering*. 4th Edn. SAE. Warrendale. PA.

Islam, M., Decker, F., de Villiers, E., Jackson, A., Gines, J., Grahs, T., Gitt-Gehrke, A. and Comas I Font, J. (2009). Application of detached-eddy simulation for automotive aerodynamics development. *SAE Paper No.* 2009-01-0333.

Kang, S. O., Jun, S. O., Park, H. I., Ku, Y. C., Kee, J. D., Kim, K. H. and Lee, D. H. (2009). CFD flow simulation and aerodynamic performance prediction around 3-D automobile configuration represented by vehicle modeling function. *Annual Conf. Proc.*, *Korean Society of Automotive Engineers*, 1306–1312.

Kang, S. O., Jun, S. O., Park, H. I., Ku, Y. C., Kee, J. D., Kim, K. H. and Lee, D. H. (2010). Influence of rotating wheel and moving ground condition to aerodynamic performance of 3-dmensional automobile configuration. *Trans. Korean Society of Automotive Engineers* **18**, **5**, 100–107.

Kang, S. O., Jun, S. O., Park, H. I., Ku, Y. C., Kee, J. D., Kim, K. H. and Lee, D. H. (2010). Aerodynamic design optimization of automotive vehicle configuration represented by vehicle modeling function for controlling COANDA flow. *World Automotive Cong.*, *FISITA*, *No*. B-060.

Kapadia, S., Roy, S. and Wurtzler, K. (2003). Detached eddy simulation over a reference ahmed car model. *41st Aerospace Sciences Meeting and Exhibit*, AIAA-2003-0857.

Kee, J. D., Kim, M. S. and Lee, B. C. (2001). The COANDA flow control and newtonian concept approach to achieve drag reduction of a passenger vehicle. *SAE Paper No.* 2001-01-1267.

Leclerc, C. and Levallois, E. (2006). Aerodynamic drag reduction by synthetic Jet: A 2D numerical study around a simplified car. *3rd AIAA Flow Control Conf.*, 2006–3337.

Le Good, G., Howell, J., Passmore, M. and Cogotti, A. (1998). A comparison of on-road aerodynamic drag measurements with wind tunnel data from pininfarina and MIRA. *SAE Paper No.* 980394.

Potthoff, J. (1982). The aerodynamic layout of UNICAR research vehicle. *Int. Symp. Vehicle Aerodynamics, Wolfsburg.*

Rho, J. H., Ku, Y. C., Kee, J. D. and Lee, D. H. (2009). Development of vehicle modeling function for three-dimensional shape optimization. *J. Mechanical Design*, *Trans. ASME* **131**, **12**, 121004.

Rho, J. H., Ku, Y. C., Yun, S. H. and Lee, D. H. (2008). Representation of 3 dimensional automobile configurations with vehicle modeling function for a shape optimization. *Proc. KSME* 2008 *Fall Annual Meeting*, *KSME.*

Rho, J. H., Ku, Y. C., Lee, D. H., Kee, J. D. and Kim, K. Y. (2009). Application of functional design method to road vehicle aerodynamic optimization in initial design stage. *SAE Paper No.* 2009-01-1166.

Singh, R. (2003). Automated aerodynamic design optimization process for automotive vehicle. *SAE Paper No.* 2003-01-0993.

Singh, S. N., Rai, L., Puri, P. and Bhatnagar, A. (2004). Effect of moving surface on the aerodynamic drag of road vehicles. *Proc. IMechE.*, **219** *Part D: J. Automobile Engineering.*

Song, J., Yoshioka, S., Kato, T. and Kohama, Y. (2006). Characteristics of flow behind a passenger vehicle. *SAE Paper No.* 2006-01-1030.

Song, K. S., Kang, S. O., Park, H. I., Kee, J. D., Kim, K. H. and Lee, D. H. (2010). External flow simulation of a passenger car for drag reduction. *Annual Conf. Proc.*, *Korean Society of Automotive Engineers*, 1116–1125.

Song, K. S., Kang, S. O., Jun, S. O., Park, H. I., Kee, J. D., Kim, K. H. and Lee, D. H. (2011). Effects on aerodynamic drag reduction of a passenger car by rear body shape modifications. *Trans. Korean Society of Automotive Engineers* **19**, **4**, 137–145.

Spalart, P. R., Jou, W. H., Strelets, M. and Allmaras, S. R. (1997). Comments on the feasibility of LES for wings, and on a hybrid RANS/LES approach. *1st AFOSR Int. Conf. DNS/LES*, Ruston, LA. In: Advances in DNS/LES, C. Liu and Z. Liu Eds., Greyden Press, Columbus, OH, USA.

Yun, S. H. (2004). *Numerical Study of the Crosswind Safety on Korean Tilting Train Express*. M. S. Thesis. Seoul National University. Seoul. Korea.

Wassen, E., Eichinger, S. and Thiele, F. (2010). Simulation of active drag reduction for a square-back vehicle. *Notes on Numerical Fluid Mechanics and Multidisciplinary Design*, **108**, *Active Flow Control II*, 241–255.

www.nrel.gov file:///F:/09_Fuel%20Efficiency/ADVISOR 2002/documentation/advisor_doc.htm.